

ECRH deposition profile in ASDEX Upgrade

F.Leuterer, K.Kirov, G.Pereverzev, E.Poli, F.Ryter, D.Wagner

Max Planck Institut für Plasmaphysik, Euratom Association, D-85748 Garching,
Germany
e-mail: leuterer@ipp.mpg.de

The ASDEX Upgrade ECRH system is designed for very narrow power deposition. We describe different attempts to verify the deposition profile: from switch-on/off events, from modulated heating, and from simulations of pulses.

Introduction

In ASDEX Upgrade we use 140 GHz and the strongly damped second harmonic x-mode. Four ECRH beams are launched from mirrors in the torus midplane on the low field side. They are designed for narrow power deposition, even in off-axis cases when the beam is launched with a poloidal angle. This is achieved by a mixture of $\approx 90\%$ HE11 mode and $\approx 10\%$ HE12 mode in the feeding waveguides, and for two beams by additional focusing. In the plasma are approximately Gaussian with $1/e$ half width of their intensity at the waist of $w = 15$ mm for two beams and of $w = 29$ mm for the other two beams, located near the plasma centre for horizontal launching. These widths were experimentally verified by low power tests in the laboratory, but not in high power tests with the actual gyrotron beams.

For deposition calculations we use the TORBEAM code [1,2] which includes actual plasma parameters with the equilibrium magnetic field, refraction effects and takes into account the Gaussian beam shape. The deposition profiles depend on the location of the absorption volume. At small poloidal launching angle the beam crosses the absorbing flux surface nearly perpendicularly leading to narrow profiles with w of a few millimeters (averaged over a flux surface), while for large poloidal angles the beam can even be tangential to the flux surface and w can be as high as 20 mm. This is valid for beam launching with zero toroidal angle. At nonzero toroidal angle the deposition profile width increases.

We have tried to verify the deposition profiles by evaluation of switch-on/off events, by modulated power deposition and comparison with a simple analytical model, and by simulation of measurements with the ASTRA transport code. The electron temperature is measured with the ECE diagnostic which provides 60

channels with a distance of 10 - 30 mm between each other, a spatial resolution of ≈ 10 mm, and a time resolution of ≈ 30 μ sec.

Profile of dT/dt at switch-on/off

The evaluation of switch-on/off events was already described in [3], where we found that the dT/dt profiles, measured on the low field side while the actual deposition was on the field side of a flux surface, are broader than the calculated ones. However, the time required for the determination of dT/dt was much longer than the characteristic time for diffusion, $\tau = 3w^2/8\chi$, which can be as short as a few tens of μ sec for narrow profiles, and therefore the measured profiles were always broader than the calculated ones.

Profile width evaluation from modulated deposition

In cases of modulated ECRH the profile of the temperature modulation reflects the deposition profile only if the modulation frequency is very high and broadening due to diffusion can be neglected [4], which is related to the short characteristic time for diffusion and depends on the width w . The temperature modulation is then very low and comparable to the noise. At lower modulation frequency the deposition profile can also be deduced from the frequency dependence of the temperature modulation in the deposition centre, using a simple analytical model for heat diffusion in plane geometry with constant coefficients [5]. In this case the temperature modulation in the deposition centre is

$$\tilde{T}_e(x=0, t) = \tilde{T}_{e0} \cdot F(z) \cdot \exp(-i\omega t) \quad (1)$$

$$\text{with } F(z) = (-i)\pi z \exp(-i\pi z^2/2) [(1+i)/2 - C(z) - iS(z)], \\ \tilde{T}_{e0} = iP/(3n_e \sqrt{\pi\omega\mu w/2}), \quad z = w\sqrt{3\omega\mu/4\pi\chi}, \quad \text{and } \mu = 1 + ib/\omega.$$

$C(z)$ and $S(z)$ are Fresnel integrals, P is the power per unit area, and b is a damping term which we can neglect here [5]. The effect of diffusion on $\tilde{T}(x=0)$ is contained in the function $F(z)$, which is shown in Fig.1. Diffusion is negligible only for large values of z , i.e. high enough modulation frequency, where $|F(z)|$ approaches to 1 and the phase becomes 90° . At lower frequency $F(z)$ has to be taken into account.

We deposited modulated ECRH into a region with low heat diffusivity χ , realised by off-axis cw ECRH heating, where χ is reduced in the central region

due to the lower heat flux [6]. Amplitude and phase of $\tilde{T}(x=0)$ from a fast Fourier transform are shown in Fig.2. A fit of equ. (1) to the experimental data resulted in $w = 0.023$ m, whereas the TORBEAM result was $w = 0.013$ m.

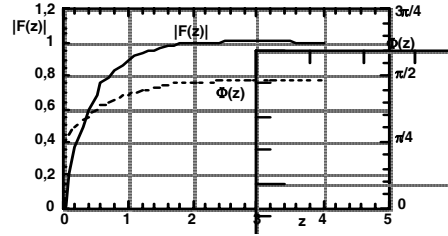


Fig.1: $|F(z)|$ and phase $\Phi(z)$ of $\tilde{T}(x=0)$. no damping $b=0$.

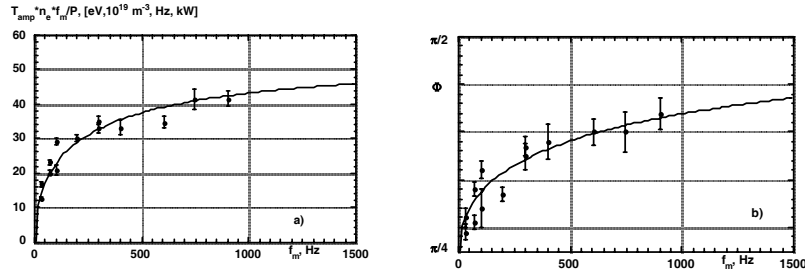


Fig.2: modulation frequency scan with narrow deposition in a low diffusivity region; a) normalised amplitude, and b) phase Φ of $\tilde{T}(x=0)$. Lines: fit to $F(z)$

A similar series was performed with a broader deposition profile (by launching with a toroidal angle of 17°) and resulted in $w = 0.043$ m, while the TORBEAM result for this case was $w = 0.025$ m.

The question did arise whether a plane geometry model is appropriate. In a paper by X.L.Zou et al. [7] the switch-on was analysed in cylindrical geometry, also with constant coefficients. We did extend this analysis to the case with modulated deposition. The result is

$$\tilde{T}_e(r,t) = \tilde{T}_{e0} \cdot G(r, r_{dep}, a, w, \chi, \omega, b) \cdot \exp(-i\omega t) \quad (2)$$

where

$$G(r, r_{dep}, a, w, \chi, \omega, b) = 2 \sum_{n=1}^{\infty} \frac{J_0(r/a \cdot \alpha_n)}{J_1^2(\alpha_n)} \cdot I_{sp}(\alpha_n, w, r_{dep}) \cdot 1/(1 - i \frac{2\chi\alpha_n^2}{a^2\omega\mu})$$

$$I_{sp}(\alpha_n, w, r_{dep}) = a^2 \int_0^1 (r'/a) J_0(r' \alpha_n / a) e^{-(r'/a - r_{dep}/a)^2 / (w/a)^2} d(r'/a) \quad \text{and}$$

$$T_{e0} = iP / (3n_e \pi \sqrt{\pi} w r_{dep} \omega \mu). \quad \text{The values of } \alpha_n \text{ are the zeroes of the Besselfunction } J_0.$$

At the deposition centre $r = r_{dep}$, equ.(2) is equivalent to equ.(1). In Fig.3 we compare the function $G(r = r_{dep}, a, w, \chi, \omega, b)$ with the function $F(z)$ of the plane geometry solution of equ.(1). Both are plotted versus the parameter $z = w\sqrt{3\omega\mu/4\pi\chi}$. Although G cannot be expressed explicitly in terms of z , both functions are identical as long as the amplitude of the generated heat wave is sufficiently low when it arrives at the centre $r = 0$ or at the edge $r = a$. In Fig.3 this is violated for $z \leq 0.07$. In our experiments described above we deposit at $\rho_{tor} \approx 0.45$ and these boundary effects are important only for modulation frequencies < 30 Hz which we did not use. This is in agreement with results in [8].

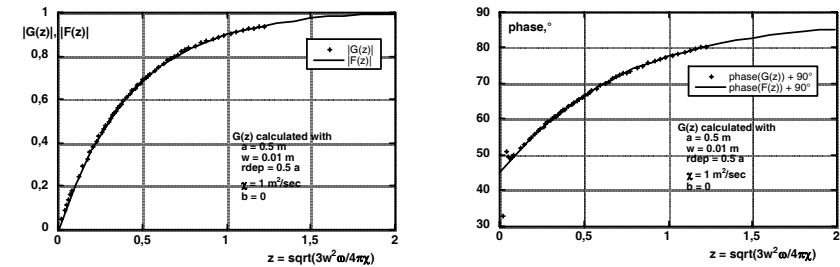


Fig.3 Comparison of the function $G(z)$ for cylindrical geometry (dots) and the function $F(z)$ for plane geometry (line), calculated for deposition at $r_{dep}/a = 0.5$. The functions are different only for very low values of z .

These plane and cylindrical models assume constant heat diffusivity χ . The effect of a gradient in χ on the temperature modulation in the deposition centre, as known for propagating heat waves [8], remains uncertain. We estimated that the higher diffusive drain of heat to one side is practically compensated by a lower drain to the other side and the effect on $\tilde{T}(x=0)$ should be very small.

Profile determination from simulations with a transport code

In a further attempt to confirm the narrow deposition profile we compared simulations with the ASTRA code with actually measured data [9]. Gradients in the parameters are then included, but we have to assume a specific model for the diffusivity. We chose the turbulent transport diffusivity of Weiland [10]. In the simulations, fitted to the measured temperature profile before applying ECRH we assume different width of the power deposition profile and look for the result that best fits the data. Fig.4 shows the temperature variation following the switch-on/off event. The dots are the measurements and the line shows the simulation. From these curves we conclude on $w \approx 0.02$ m, while the TORBEAM result for this pulse was $w = 0.011$ m.

Similarly we did simulate a modulated pulse out of the series which were evaluated in Fig.2. The amplitude of the modulated temperature profile as obtained from a fast Fourier transformation is compared in Fig.5 with the simulation result. Again we find that $w \approx 0.02$ m fits best to the data, while the TORBEAM result for this pulse was $w = 0.013$ m.

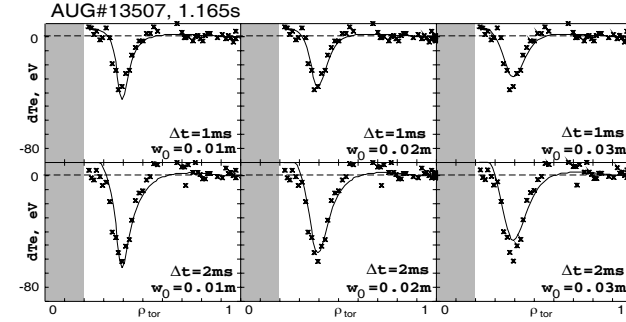
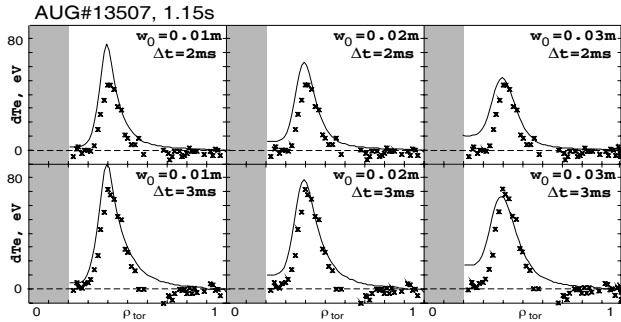


Fig.4: Comparison of experimental and simulated temperature variation $dT_e(\rho)$ for 3 different values of deposition profile width $w = 0.01, 0.02$ and 0.03 m. top) 2 and 3 msec after switch-on ECRH. bottom) 1 and 2 msec after switch-off.

Fig.5: Experimental $\tilde{T}_e(\rho)$ profiles from FFT (dots) compared to calculated profiles from ASTRA (full lines) assuming deposition profiles (dashed lines) of different width $w = 0.01, 0.02$ and 0.03 m. $f_{\text{mod}} = 300$ Hz.

Summary

We described various methods to derive the ECRH power deposition profile in ASDEX Upgrade: measuring dT/dt after switch-on/off of the heating pulse, evaluation of the temperature modulation in the deposition centre for modulated ECRH, and simulation of pulses with a transport code. All attempts resulted in a deposition profile which is a factor 1.5 to 2 wider than that calculated with our TORBEAM code. Such a code of course assumes an instantaneous distribution of the heat across a flux surface, whereas in fact this will need some time. For very narrow profiles this time can be comparable or even larger than the

characteristic time for diffusion. Measurements leading to an effective profile will therefore always give broader profiles than the calculated ones. We also have to mention that the actual high power beam must not necessarily have the properties of a low power test beam.

References

- [1] Poli E. et al., Phys. Plasmas 6 (1999) 5
- [2] Poli E. et al., Comput. Phys. Commun. 136 (2001) 90
- [3] Leuterer F. et al., Europhysics Conf. Abstr. 21A (1997), Vol.IV, 1533
- [4] Erckmann V. et al., Plasma Phys. Contr. Fusion 36 (1994) 1869
- [5] Leuterer F. et al., Nucl. Fusion 43 (2003) 744
- [6] Ryter F., et al., Phys. Rev. Lett 86 (2001) 2325
- [7] Zou X.L. et al., Nucl. Fusion 43 (2003) 1411
- [8] Jacchia A. et al., Phys. Fluids B3 (1991) 3033
- [9] Kirov K. et al., Plasma Phys. Contr. Fusion 44 (2002) 2583
- [10] Nordmann H. et al., Nucl. Fusion 30 (1990) 983